

Research Article

Conformal Mapping of Unbounded Multiply Connected Regions onto Canonical Slit Regions

**Arif A. M. Yunus,^{1,2,3} Ali H. M. Murid,^{1,2} and
Mohamed M. S. Nasser^{4,5}**

¹ Department of Mathematical Sciences, Faculty of Science, Universiti Teknologi Malaysia, Johor, 81310 Johor Bahru, Malaysia

² Ibnu Sina Institute for Fundamental Science Studies, Universiti Teknologi Malaysia, Johor, 81310 Johor Bahru, Malaysia

³ Faculty of Science and Technology, Universiti Sains Islam Malaysia, Negeri Sembilan 71800, Bandar Baru Nilai, Malaysia

⁴ Department of Mathematics, Faculty of Science, King Khalid University, P.O. Box 9004, Abha, Saudi Arabia

⁵ Department of Mathematics, Faculty of Science, Ibb University, P. O. Box 70270, Ibb, Yemen

Correspondence should be addressed to Ali H. M. Murid, alihassan@utm.my

Received 22 May 2012; Accepted 18 July 2012

Academic Editor: Matti Vuorinen

Copyright © 2012 Arif A. M. Yunus et al. This is an open access article distributed under the Creative Commons Attribution License, which permits unrestricted use, distribution, and reproduction in any medium, provided the original work is properly cited.

We present a boundary integral equation method for conformal mapping of unbounded multiply connected regions onto five types of canonical slit regions. For each canonical region, three linear boundary integral equations are constructed from a boundary relationship satisfied by an analytic function on an unbounded multiply connected region. The integral equations are uniquely solvable. The kernels involved in these integral equations are the modified Neumann kernels and the adjoint generalized Neumann kernels.

1. Introduction

In this paper, we present a new method for numerical conformal mapping of unbounded multiply connected regions onto five types of canonical slit regions. A canonical region in conformal mapping is known as a set of finitely connected regions S such that each finitely connected nondegenerate region is conformally equivalent to a region in S . With regard to conformal mapping of multiply connected regions, there are several types of canonical regions as listed in [1–4]. The five types of canonical slit regions are disk with

concentric circular slits U_d , annulus with concentric circular slits U_a , circular slit regions U_c , radial slit regions U_r , and parallel slit regions U_p . One major setback in conformal mapping is that only for certain regions exact conformal maps are known. One way to deal with this limitation is by numerical computation. Trefethen [5] has discussed several methods for computing conformal mapping numerically. Amano [6] and DeLillo et al. [7] have successfully map unbounded regions onto circular and radial slit regions. Boundary integral equation related to a boundary relationship satisfied by a function which is analytic in a simply or doubly connected region bounded by closed smooth Jordan curves has been given by Murid [8] and Murid and Razali [9]. Special realizations of this integral equation are the integral equations related to the Szegő kernel, Bergmann kernel, Riemann map, and Ahlfors map. The kernels arise in these integral equations are the Neumann kernel and the Kerzman-Stein kernel. Murid and Hu [10] managed to construct a boundary integral equation for numerical conformal mapping of a bounded multiply connected region onto a unit disk with slits. However, the integral equation involves unknown radii which lead to a system of nonlinear algebraic equations upon discretization of the integral equation. Nasser [11–13] produced another technique for numerical conformal mapping of bounded and unbounded multiply connected regions by expressing the mapping function in terms of the solution of a uniquely solvable Riemann-Hilbert problem. This uniquely solvable Riemann Hilbert problem can be solved by means of boundary integral equation with the generalized Neumann kernel. Recently, Sangawi et al. [14–17] have constructed new linear boundary integral equations for conformal mapping of bounded multiply region onto canonical slit regions, which improves the work of Murid and Hu [10] where in [10], the system of algebraic equations are nonlinear. In this paper, we extend the work of [14–17] for numerical conformal mapping of unbounded multiply connected regions onto all five types of canonical slit regions. These boundary integral equations are constructed from a boundary relationship satisfied by an analytic function on an unbounded multiply connected region.

The plan of this paper is as follows: Section 2 presents some auxiliary material. Section 3 presents a boundary integral equation related to a boundary relationship. In Sections 4–8, we present the derivations for numerical conformal mapping for all five types of canonical regions. In Section 9, we give some examples to illustrate the effectiveness of our method. Finally, Section 10 presents a short conclusion.

2. Auxiliary Material

Let Ω^- be an unbounded multiply connected region of connectivity m . The boundary Γ consists of m smooth Jordan curves Γ_j , $j = 1, 2, \dots, m$ and will be denoted by $\Gamma = \Gamma_1 \cup \Gamma_2 \cup \dots \cup \Gamma_m$. The boundaries Γ_j are assumed in clockwise orientation (see Figure 1). The curve Γ_j is parameterized by 2π -periodic twice continuously differentiable complex function $\eta_j(t)$ with nonvanishing first derivative, that is,

$$\eta'_j(t) = \frac{d\eta_j(t)}{dt} \neq 0, \quad t \in J_j = [0, 2\pi], \quad k = 1, \dots, m. \quad (2.1)$$

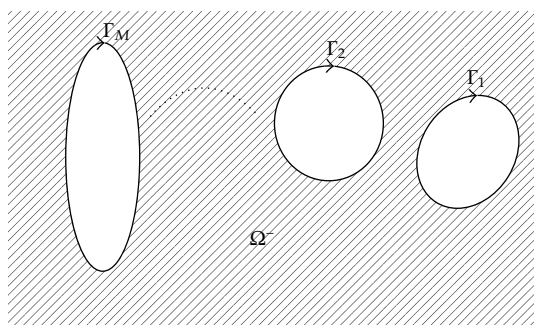


Figure 1: An unbounded multiply connected region Ω^- with connectivity m .

The total parameter domain J is the disjoint union of m intervals J_1, \dots, J_m . We define a parameterization η of the whole boundary Γ on J by

$$\eta(t) = \begin{cases} \eta_1(t), & t \in J_1 = [0, 2\pi], \\ \vdots \\ \eta_m(t), & t \in J_m = [0, 2\pi]. \end{cases} \tag{2.2}$$

Let $\Phi(z)$ be the conformal mapping function that maps Ω^- onto U^- , where U^- represents any canonical region mentioned above, z_1 is a prescribed point located inside Γ_1 , z_m is a prescribed point inside Γ_m and β is a prescribed point located in Ω^- . In this paper, we determine the mapping function $\Phi(z)$ by computing the derivatives of the mapping function $\Phi'(\eta(t))$ and two real functions on J , that is, the unknown function $\varphi(t)$ and a piecewise constant real function $R(t)$. Let H be the space of all real Hölder continuous 2π -periodic functions and S be the subspace of H which contains the piecewise real constant functions $R(t)$. The piecewise real constant function $R(t)$ can be written as

$$R(t) = \begin{cases} R_1, & t \in J_1 = [0, 2\pi], \\ \vdots \\ R_m, & t \in J_m = [0, 2\pi], \end{cases} \tag{2.3}$$

briefly written as $R(t) = (R_1, \dots, R_m)$. Let $A(t)$ be a complex continuously differentiable 2π -periodic function for all $t \in J$. We define two real kernels formed with A as [18]

$$\begin{aligned} N(s, t) &= \frac{1}{\pi} \operatorname{Im} \left(\frac{A(s)}{A(t)} \frac{\eta'(t)}{\eta(t) - \eta(s)} \right), \\ M(s, t) &= \frac{1}{\pi} \operatorname{Re} \left(\frac{A(s)}{A(t)} \frac{\eta'(t)}{\eta(t) - \eta(s)} \right). \end{aligned} \tag{2.4}$$

The kernel $N(s, t)$ is known as the generalized Neumann kernel formed with complex-valued functions A and η . The kernel $N(s, t)$ is continuous with

$$N(t, t) = \frac{1}{\pi} \operatorname{Im} \left(\frac{\eta''(t)}{\eta'(t)} - \frac{A'(t)}{A(t)} \right). \quad (2.5)$$

The kernel $M(s, t)$ has a cotangent singularity

$$M(s, t) = -\frac{1}{2\pi} \cot \frac{s-t}{2} + M_1(s, t), \quad (2.6)$$

where the kernel $M_1(s, t)$ is continuous with

$$M_1(t, t) = \frac{1}{\pi} \operatorname{Re} \left(\frac{1}{2\pi} \frac{\eta''(t)}{\eta'(t)} - \frac{A'(t)}{A(t)} \right). \quad (2.7)$$

The adjoint function \tilde{A} of A is defined by

$$\tilde{A} = \frac{\eta'(t)}{A(t)}. \quad (2.8)$$

The generalized Neumann kernel $\tilde{N}(s, t)$ and the real kernel \tilde{M} formed with \tilde{A} are defined by

$$\begin{aligned} \tilde{N}(s, t) &= \frac{1}{\pi} \operatorname{Im} \left(\frac{\tilde{A}(s)}{\tilde{A}(t)} \frac{\eta'(t)}{\eta(t) - \eta(s)} \right), \\ \tilde{M}(s, t) &= \frac{1}{\pi} \operatorname{Re} \left(\frac{\tilde{A}(s)}{\tilde{A}(t)} \frac{\eta'(t)}{\eta(t) - \eta(s)} \right). \end{aligned} \quad (2.9)$$

Then,

$$\tilde{N}(s, t) = -N^*(s, t), \quad \tilde{M}(s, t) = -M^*(s, t), \quad (2.10)$$

where $N^*(s, t) = N(t, s)$ is the adjoint kernel of the generalized Neumann kernel $N(s, t)$. We define the Fredholm integral operators \mathbf{N}^* by

$$\mathbf{N}^*v(t) = \int_J N^*(t, s)v(s)ds, \quad t \in J. \quad (2.11)$$

Integral operators M^* , \tilde{N} , and \tilde{M} are defined in a similar way. Throughout this paper, we will assume the functions A and \tilde{A} are given by

$$A(t) = 1, \quad \tilde{A}(t) = \eta'(t). \quad (2.12)$$

It is known that $\lambda = 1$ is not an eigenvalue of the kernel N and $\lambda = -1$ is an eigenvalue of the kernel N with multiplicity m [18]. The eigenfunctions of N corresponding to the eigenvalue $\lambda = -1$ are $\{\chi^{[1]}, \chi^{[2]}, \dots, \chi^{[m]}\}$, where

$$\chi^{[j]}(\xi) = \begin{cases} 1, & \xi \in \Gamma_j, \\ 0, & \text{otherwise.} \end{cases} \quad j = 1, 2, \dots, m. \quad (2.13)$$

We also define an integral operator J by (see [14])

$$J\mu(s) := \int_J \frac{1}{2\pi} \sum_{j=0}^m \chi^{[j]}(s) \chi^{[j]}(t) \mu(t) dt. \quad (2.14)$$

The following theorem gives us a method for calculating the piecewise constant real function $h(t)$ in connection with conformal mapping later. This theorem can be proved by using the approach as in [19, Theorem 5].

Theorem 2.1. *Let $i = \sqrt{-1}$, $\gamma, \mu \in H$ and $h \in S$ such that*

$$Af = \gamma + h + i\mu \quad (2.15)$$

are the boundary values of a function $f(z)$ analytic in Ω^- . Then the function $h = (h_1, h_2, \dots, h_m)$ has each element given by

$$h_j = (\gamma, \rho^{[j]}) = \frac{1}{2\pi} \int_{\Gamma} \gamma(t) \rho^{[j]} dt, \quad (2.16)$$

where $\rho^{[j]}$ is the unique solution of the integral equation

$$(\mathbf{I} + \mathbf{N}^* + \mathbf{J})\rho^{[j]} = -\chi^{[j]}, \quad j = 1, 2, \dots, m. \quad (2.17)$$

3. The Homogeneous Boundary Relationship

Suppose we are given a function $D(z)$ which is analytic in Ω^- , continuous on $\Omega^- \cup \Gamma$, Hölder continuous on Γ and $D(\infty)$ is finite. The boundary Γ_j is assumed to be a smooth Jordan curve. The unit tangent to Γ at the point $\eta(t) \in \Gamma$ will be denoted by $T(\eta(t)) = \eta'(t)/|\eta'(t)|$. Suppose further that $D(\eta(t))$ satisfies the exterior homogeneous boundary relationship

$$D(\eta(t)) = c(t) \frac{\overline{T(\eta(t))}^2 \overline{D(\eta(t))}}{P(\eta(t))}, \quad (3.1)$$

where $c(t)$ and P are complex-valued functions with the following properties:

- (1) $P(z)$ is analytic in Ω^- and does not have zeroes on $\Omega^- \cup \Gamma$,
- (2) $P(\infty) \neq 0$, $D(\infty)$ is finite,
- (3) $c(t) \neq 0$, $P(\eta(t)) \neq 0$.

Note that the boundary relationship (3.1) also has the following equivalent form:

$$P(\eta(t)) = \overline{c(t)}T(\eta(t))^2 \frac{D(\eta(t))^2}{|D(\eta(t))|^2}. \quad (3.2)$$

Under these assumptions, an integral equation for $D(\eta(t))$ can be constructed by means of the following theorem.

Theorem 3.1. *If the function $D(\eta(t))$ satisfies the exterior homogeneous boundary relationship (3.1), then*

$$\phi(t) + \int_J K(s,t)\phi(s)ds = v(t), \quad (3.3)$$

where

$$\begin{aligned} \phi(t) &= D(\eta(t))\eta'(t), \\ K(s,t) &= \frac{1}{2\pi i} \left[\frac{\eta'(t)}{\eta(t) - \eta(s)} - \frac{c(t)}{c(s)} \frac{\overline{\eta'(t)}}{\overline{(\eta(t) - \eta(s))}} \right], \\ v(t) &= D(\infty)\eta'(t) + c(t)\eta'(t) \frac{\overline{D(\infty)}}{P(\infty)}. \end{aligned} \quad (3.4)$$

Proof. Consider the integral $I_1(\eta(t))$,

$$I_1(\eta(t)) = \frac{1}{2\pi i} \int_J \frac{D(\eta(s))}{\eta(s) - \eta(t)} ds. \quad (3.5)$$

Since the boundary is in clockwise orientation and D is analytic in Ω^- , then by [20, p. 2] we have

$$I_1(\eta(t)) = \frac{D(\eta(t))}{2} - D(\infty). \quad (3.6)$$

Now, let the integral $I_2(\eta(t))$ be defined as

$$I_2(\eta(t)) = \frac{1}{2\pi i} \int_J \frac{c(t)\overline{T(\eta(t))}^2 D(\eta(s))}{c(s)(\eta(s) - \eta(t))\overline{T(\eta(s))}} |ds|. \quad (3.7)$$

Using the boundary relationship (3.1) and the fact that $\overline{T(\eta(t))}|dt| = dt$ and $P(\eta(t))$ does not contain zeroes, then by [20, p. 2] we obtain

$$I_2(\eta(t)) = -c(t)\overline{T(\eta(t))}^2\frac{\overline{D(\eta(t))}}{P(\eta(t))} + c(t)\overline{T(\eta(t))}^2\frac{\overline{D(\infty)}}{P(\infty)}. \tag{3.8}$$

Next, by taking $I_2(\eta(t)) - I_1(\eta(t))$ with further arrangement yields

$$\begin{aligned} D(\eta(t)) + \frac{1}{2\pi i} \int_J \left[\frac{1}{\eta(t) - \eta(s)} - \frac{c(t)}{c(s)} \frac{\overline{T(\eta(t))}^2}{\eta(t) - \eta(s)} \right] D(\eta(s)) |ds| \\ = D(\infty) + c(t)\overline{T(\eta)}^2\frac{\overline{D(\infty)}}{P(\infty)}. \end{aligned} \tag{3.9}$$

Then multiplying (3.9) with $T(\eta(t))$ and $|\eta'(t)|$, subsequently yields (3.3). □

Theorem 3.2. *The kernel $K(s, t)$ is continuous with*

$$K(t, t) = \frac{1}{2\pi} \operatorname{Im} \frac{\eta''(t)}{\eta'(t)} - \frac{1}{2\pi i} \frac{c'(t)}{c(t)}. \tag{3.10}$$

Proof. Let the kernel $K(s, t)$ be written as

$$K(s, t) = K_1(s, t) + K_2(s, t), \tag{3.11}$$

where

$$\begin{aligned} K_1(s, t) &= \frac{1}{2\pi i} \left[\frac{\eta'(t)}{\eta(t) - \eta(s)} - \frac{\overline{\eta'(t)}}{\eta(t) - \eta(s)} \right], \\ K_2(s, t) &= \frac{1}{2\pi i} \left[-\frac{c(t)}{c(s)} \frac{\overline{\eta'(t)}}{\eta(t) - \eta(s)} + \frac{\overline{\eta'(t)}}{\eta(t) - \eta(s)} \right] = \frac{1}{2\pi i} \frac{\overline{\eta'(t)}}{c(s)} \left[\frac{c(s) - c(t)}{\eta(t) - \eta(s)} \right]. \end{aligned} \tag{3.12}$$

Notice that $K_1(s, t)$ is the classical Neumann kernel with $K_1(t, t) = 1/(2\pi) \operatorname{Im}((\eta''(t))/(\eta'(t)))$. Now for $K_2(s, t)$, as we take the limit $s \rightarrow t$ we have,

$$\begin{aligned} K_2(t, t) &= \frac{1}{2\pi i} \lim_{s \rightarrow t} \frac{\overline{\eta'(t)}}{c(s)} \lim_{s \rightarrow t} \left[\frac{c(s) - c(t)}{\eta(t) - \eta(s)} \right] \\ &= -\frac{1}{2\pi i} \frac{c'(t)}{c(t)}. \end{aligned} \tag{3.13}$$

Hence, by combining $K_1(t, t)$ and $K_2(t, t)$, we obtain

$$K(t, t) = \frac{1}{2\pi} \left(\operatorname{Im} \frac{\eta''(t)}{\eta'(t)} - \frac{1}{i} \frac{c'(t)}{c(t)} \right). \quad (3.14)$$

□

Note that when $c(t) = 1$, the kernel $K(s, t)$ reduces to the classical Neumann kernel.

We define the Fredholm integral operator \mathbf{K} by

$$\mathbf{K}v(t) = \frac{1}{2\pi i} \int_J K(s, t)v(s)ds, \quad t \in J. \quad (3.15)$$

Hence, (3.3) becomes

$$(\mathbf{I} + \mathbf{K})\phi(t) = v(t). \quad (3.16)$$

The solvability of the integral equation (3.16) depends on the possibility of $\lambda = -1$ being an eigenvalue of the kernel $K(s, t)$. For the numerical examples considered in this paper, $\lambda = -1$ is always an eigenvalue of the kernel $K(s, t)$. Although there is no theoretical proof yet, numerical evidence suggests that $\lambda = -1$ is an eigenvalue of $K(s, t)$. If the multiplicity of the eigenvalue $\lambda = -1$ is \widehat{m} , then one need to add \widehat{m} conditions to the integral equation to ensure the integral equation is uniquely solvable.

4. Exterior Unit Disk with Circular Slits

The canonical region U_d is the exterior unit disk along with $m - 1$ arcs of circles. We assume that $w = \Phi(z)$ maps the curve Γ_1 onto the unit circle $|w| = 1$, the curve Γ_j , where $j = 2, 3, \dots, m$, onto circular slit on the circle $|w| = R_j$, where R_2, R_3, \dots, R_m are unknown real constants. The circular slits are traversed twice. The boundary values of the mapping function Φ are given by

$$\Phi(\eta(t)) = R(t)e^{i\theta(t)}, \quad (4.1)$$

where $\theta(t)$ represents the boundary correspondence function and $R(t) = (1, R_2, \dots, R_m)$. By differentiating (4.1) with respect to t and dividing the result obtained by its modulus, we have

$$\frac{\Phi'(\eta(t))\eta'(t)}{|\Phi'(\eta(t))\eta'(t)|} = i \operatorname{sign}(\theta'(t))e^{i\theta(t)}. \quad (4.2)$$

Using the fact that unit tangent $T(\eta(t)) = \eta'(t)/|\eta'(t)|$ and $e^{i\theta(t)} = \Phi(\eta(t))/R(t)$, it can be shown that

$$\Phi(\eta(t)) = \operatorname{sign}(\theta'(t)) \frac{R(t)}{i} T(\eta(t)) \frac{\Phi'(\eta(t))}{|\Phi'(\eta(t))|}. \quad (4.3)$$

Boundary relationship (4.3) is useful for computing the boundary values of $\Phi(z)$ provided $\theta'(t)$, $R(t)$, and $\Phi'(\eta(t))$ are all known. By taking logarithmic derivative on (4.1), we obtain

$$\eta'(t) \frac{\Phi'(\eta(t))}{\Phi(\eta(t))} = i\theta'(t). \tag{4.4}$$

The mapping function $\Phi(z)$ can be uniquely determined by assuming

$$\Phi(\infty) = \infty, \quad c = \Phi'(\infty) = \lim_{z \rightarrow \infty} \frac{\Phi(z)}{z} > 0. \tag{4.5}$$

Thus, the mapping function can be expressed as [12]

$$\Phi(z) = c(z - z_1)e^{F(z)}, \tag{4.6}$$

where $F(z)$ is an analytic function and $F(\infty) = 0$. By taking logarithm on both sides of (4.6), we obtain

$$F(\eta(t)) = \ln \frac{R(t)}{c} + i\theta - \log(\eta(t) - z_1). \tag{4.7}$$

Hence (4.7) satisfies boundary values (2.15) in Theorem 2.1 with $A(t) = 1$,

$$h(t) = \left(\ln \frac{1}{c}, \ln \frac{R_2}{c}, \dots, \ln \frac{R_m}{c} \right), \quad \gamma(t) = -\ln|\eta(t) - z_1|. \tag{4.8}$$

Hence, the values of R_j can be calculated by

$$R_j = e^{h_j - h_1} \quad \text{for } j = 1, 2, \dots, m. \tag{4.9}$$

To find $\theta'(t)$, we began by differentiating (4.7) and comparing with (4.4) which yields

$$i\theta'(t) = F'(\eta(t))\eta'(t) - \frac{\eta'(t)}{\eta(t) - z_1}. \tag{4.10}$$

In view of $\tilde{A} = \eta'(t)$ and letting $f(z) = F'(z) - 1/(z - z_1)$, where $f(z)$ is analytic function in Ω^- , (4.10) becomes

$$\tilde{A}f(\eta(t)) = i\theta'(t). \tag{4.11}$$

By [18, Theorem 2(c)], we obtain $(\mathbf{I} - \tilde{\mathbf{N}})\theta' = 0$ which implies

$$(\mathbf{I} + \mathbf{N}^*)\theta' = 0. \tag{4.12}$$

However, this integral equation is not uniquely solvable according to [18, Theorem 12]. To overcome this, since the image of the curve Γ_1 is clockwise oriented and the images of the curves $\Gamma_j, j = 2, 3, \dots, m$ are slits so we have $\theta_1(2\pi) - \theta_1(0) = -2\pi$ and $\theta_j(2\pi) - \theta_j(0) = 0$, which implies

$$\mathbf{J}\theta'(t) = \tilde{h}(t) = (-1, 0, \dots, 0). \quad (4.13)$$

By adding this condition to (4.12), the unknown function $\theta'(t)$ is the unique solution of the integral equation

$$(\mathbf{I} + \mathbf{N}^* + \mathbf{J})\theta'(t) = \tilde{h}(t). \quad (4.14)$$

Next, the presence of $\text{sign}(\theta'(t))$ in (4.3) can be eliminated by squaring both sides of (4.3), that is,

$$\Phi(\eta(t))^2 = -R(t)^2 T(\eta(t))^2 \frac{\Phi'(\eta(t))^2}{|\Phi'(\eta(t))|^2}. \quad (4.15)$$

Upon comparing (4.15) with (3.2), this leads to a choice of $P(\eta(t)) = \Phi(\eta(t))^2, P(\infty) = \infty, D(\eta(t)) = \Phi'(\eta(t)), D(\infty) = c, c(t) = -R(t)^2$. Hence,

$$\phi(t) = \Phi'(\eta(t))\eta'(t) \quad (4.16)$$

satisfies the integral equation (3.16) with

$$\nu(t) = \Phi'(\infty)\eta'(t). \quad (4.17)$$

Numerical evidence shows that $\lambda = -1$ is an eigenvalue of $K(s, t)$ of multiplicity m , which means one needs to add m conditions. Since $\Phi(z)$ is assumed to be single-valued, it is also required that the unknown mapping function $\Phi'(z)$ satisfies [4]

$$\int_{J_j} \phi(t) dt = \int_{\Gamma_j} \Phi'(\eta) d\eta = 0, \quad j = 1, 2, \dots, m, \quad (4.18)$$

that is,

$$\mathbf{J}\phi = 0. \quad (4.19)$$

Then, $\phi(t)$ is the unique solution of the following integral equation

$$(\mathbf{I} + \mathbf{K} + \mathbf{J})\phi(t) = \nu(t). \quad (4.20)$$

By obtaining $\phi(t)$, the derivatives of the mapping function, $\Phi'(t)$ can be found using

$$\Phi'(t) = \frac{\phi'(t)}{\eta'(t)}. \tag{4.21}$$

By obtaining the values of $R(t)$, $\theta'(t)$ and $\Phi'(\eta(t))$, the boundary value of $\Phi(\eta(t))$ can be calculated by using (4.3).

5. Annulus with Circular Slits

The canonical region U_a consists of an annulus centered at the origin together with $m - 2$ circular arcs. We assume that $\Phi(z)$ maps the curve Γ_1 onto the unit circle $|\Phi| = 1$, the curve Γ_m onto the circle $|\Phi| = R_m$ and Γ_j onto circular slit $|\Phi| = R_j$, where $j = 2, 3, \dots, m - 1$. The slit are traversed twice. The boundary values of the mapping function Φ are given by

$$\Phi(\eta(t)) = R(t)e^{i\theta(t)}, \tag{5.1}$$

where $\theta(t)$ represents the boundary correspondence function and $R(t) = (1, R_2, \dots, R_m)$ is a piecewise real constant function. By using the same reasoning as in Section 4, we get

$$\Phi(\eta_j(t)) = \text{sign}(\theta'(t)) \frac{R_j(t)}{i} T(\eta_j(t)) \frac{\Phi'(\eta_j(t))}{|\Phi'(\eta_j(t))|}, \tag{5.2}$$

$$\eta'(t) \frac{\Phi'(\eta(t))}{\Phi(\eta(t))} = i\theta'(t). \tag{5.3}$$

The mapping function $\Phi(z)$ can be uniquely determined by assuming $c = \Phi(\infty) > 0$. Thus, the mapping function can be expressed as [12]

$$\Phi(z) = c \frac{z - z_m}{z - z_1} e^{F(z)}. \tag{5.4}$$

By taking logarithm on both sides of (5.4), we obtain

$$F(\eta(t)) = \ln \frac{R(t)}{c} + i\theta - \log \frac{\eta(t) - z_m}{\eta(t) - z_1}. \tag{5.5}$$

Hence, (5.5) satisfies boundary values (2.15) in Theorem 2.1 with $A(t)=1$,

$$h(t) = \left(\ln \frac{1}{c}, \ln \frac{R_2}{c}, \dots, \ln \frac{R_m}{c} \right), \quad \gamma(t) = -\ln \left| \frac{\eta(t) - z_m}{\eta(t) - z_1} \right|. \tag{5.6}$$

By obtaining h_j , the values of R_j can be computed by

$$R_j = e^{h_j - h_1}, \quad j = 2, 3, \dots, m. \tag{5.7}$$

By differentiating (5.5) and comparing with (5.3) yields

$$i\theta'(t) = F'(\eta(t))\eta'(t) + \frac{\eta'(t)}{\eta(t) - z_m} - \frac{\eta'(t)}{\eta(t) - z_1}. \quad (5.8)$$

In view of $\tilde{A} = \eta'(t)$ and $f(\eta(t)) = F'(\eta(t)) + 1/(\eta(t) - z_m) - 1/(\eta(t) - z_1)$, where $f(z)$ is analytic in Ω^- , (5.8) is equivalent to

$$\tilde{A}f(\eta(t)) = i\theta'(t). \quad (5.9)$$

By [18, Theorem 2(c)], we obtain

$$(\mathbf{I} + \mathbf{N}^*)\theta'(t) = 0. \quad (5.10)$$

Note that the image of the curve Γ_1 is counterclockwise oriented, Γ_m is clockwise oriented and the images of the curves $\Gamma_j, j = 2, 3, \dots, m-1$ are slits so we have $\theta_1(2\pi) - \theta_1(0) = 2\pi$, $\theta_m(2\pi) - \theta_m(0) = -2\pi$ and $\theta_j(2\pi) - \theta_j(0) = 0$, which implies

$$\mathbf{J}\theta'(t) = \tilde{h}(t) = (1, 0, \dots, -1). \quad (5.11)$$

Hence, the unknown function $\theta'(t)$ is the unique solution of the integral equation

$$(\mathbf{I} + \mathbf{N}^* + \mathbf{J})\theta'(t) = \tilde{h}(t). \quad (5.12)$$

Next, the presence of $\text{sign}(\theta'(t))$ in (5.2) can be eliminated by squaring both sides of the equation, that is,

$$\Phi(\eta(t))^2 = -R(t)^2 T(\eta(t))^2 \frac{\Phi'(\eta(t))^2}{|\Phi'(\eta(t))|^2}. \quad (5.13)$$

Comparing (5.13) with (3.2) leads to a choice of $P(\eta(t)) = \Phi(\eta(t))^2$, $P(\infty) = c^2$, $D(\eta(t)) = \Phi'(\eta(t))$, $D(\infty) = 0$, $c(t) = -R(t)^2$. Hence,

$$\phi(t) = \Phi'(\eta(t))\eta'(t) \quad (5.14)$$

satisfies the integral equation (3.16) with

$$\nu(t) = (0, \dots, 0). \quad (5.15)$$

Numerical evidence shows that $\lambda = -1$ is an eigenvalue of $K(s, t)$ of multiplicity $m + 1$, which implies one needs to add $m + 1$ conditions. Since $\Phi(z)$ is assumed to be single-valued, hence it is also required that the unknown mapping function $\Phi'(z)$ satisfies [4]

$$\int_{\Gamma_j} \phi(s) ds = \int_{\Gamma_j} \Phi'(\eta) d\eta = 0, \quad j = 1, 2, \dots, m, \quad (5.16)$$

that is,

$$\mathbf{J}\phi = 0. \quad (5.17)$$

Since we assume the mapping function $\Phi(z)$ can be uniquely determined by $c = \Phi(\infty) > 0$, hence by [20]

$$\Phi(\infty) = c = \frac{1}{2\pi} \int_J \frac{\eta'(t)}{\theta'(t)(\eta - z_1)} \phi(t) dt. \quad (5.18)$$

If we define the Fredholm operator \mathbf{G} as

$$\mathbf{G}\mu(s) = \frac{1}{2\pi} \int_J \frac{\eta'(t)}{\theta'(t)(\eta - z_1)} \mu(t) dt, \quad (5.19)$$

then $\phi(t)$ is the unique solution of the following integral equation:

$$(\mathbf{I} + \mathbf{K} + \mathbf{J} + \mathbf{G})\phi(t) = c. \quad (5.20)$$

By obtaining $\phi(\eta(t))$, the derivatives of the mapping function, $\Phi'(t)$ can be obtained by

$$\Phi'(t) = \frac{\phi(\eta(t))}{\eta'(t)}. \quad (5.21)$$

6. Circular Slits

The canonical region U_c consists of m slits along the circle $|\Phi| = R_j$ where $j = 1, 2, \dots, m$ and R_1, R_2, \dots, R_m are unknown real constants. The boundary values of the mapping function Φ are given by

$$\Phi(\eta(t)) = R(t)e^{i\theta(t)}, \quad (6.1)$$

where $\theta(t)$ represents the boundary correspondence function and $R(t) = (1, R_2, \dots, R_m)$. By using the same reasoning as in Section 4, we get

$$\Phi(\eta_j(t)) = \text{sign}(\theta'(t)) \frac{R_j(t)}{i} T(\eta_j(t)) \frac{\Phi'(\eta_j(t))}{|\Phi'(\eta_j(t))|}, \quad (6.2)$$

$$\eta'(t) \frac{\Phi'(\eta(t))}{\Phi(\eta(t))} = i\theta'(t). \quad (6.3)$$

The mapping function $\Phi(z)$ can be uniquely determined by assuming $\Phi(\beta) = 0$, $\Phi(\infty) = \infty$ and $\Phi'(\infty) = 1$. Thus, the mapping function Φ can be expressed as [12]

$$\Phi(z) = (z - \beta)e^{F(z)}. \quad (6.4)$$

By taking logarithm on both sides of (6.4), we obtain

$$F(\eta(t)) = \ln R(t) + i\theta - \log(\eta(t) - \beta). \quad (6.5)$$

Hence, (6.5) satisfies boundary values in Theorem 2.1 with $A(t) = 1$,

$$h(t) = (\ln R_1, \ln R_2, \dots, \ln R_m), \quad \gamma(t) = -\ln|\eta(t) - \beta|. \quad (6.6)$$

By obtaining h_j , the values of R_j can be obtained by

$$R_j = e^{h_j}. \quad (6.7)$$

By differentiating (6.5) and comparing with (6.3) yields

$$i\theta'(t) = F'(\eta(t))\eta'(t) + \frac{\eta'(t)}{\eta(t) - \beta}. \quad (6.8)$$

In view of $\tilde{A} = \eta'(t)$, $f(t) = F'(\eta(t))$ and $g(t) = 1/(\eta(t) - \beta)$ where $f(z)$ is analytic in Ω^- and $g(z)$ is analytic in Ω^+ , we rewrite (6.8) as

$$\tilde{A}f(\eta(t)) = i\theta'(t) - \tilde{A}g(\eta(t)). \quad (6.9)$$

Let $\tilde{A}g(t) = \varphi + i\psi$. Then by [18, Theorems 2(c) and 2(d)], we obtain

$$(\mathbf{I} + \mathbf{N}^*)(\theta'(t) - \varphi(t)) = \tilde{\mathbf{M}}\varphi(t), \quad (6.10)$$

$$(\mathbf{I} - \mathbf{N}^*)\varphi(t) = \tilde{\mathbf{M}}\varphi(t). \quad (6.11)$$

Subtracting (6.11) from (6.10), we get

$$(\mathbf{I} + \mathbf{N}^*)\theta'(t) = 2\varphi(t). \tag{6.12}$$

Since the images of the curve $\Gamma_1, \Gamma_2, \dots, \Gamma_m$ are slits, we have $\theta_j(2\pi) - \theta_j(0) = 0$. Thus

$$\mathbf{J}\theta'(t) = (0, 0, \dots, 0). \tag{6.13}$$

Hence the unknown function $\theta'(t)$ is the unique solution of the integral equation

$$(\mathbf{I} + \mathbf{N}^* + \mathbf{J})\theta'(t) = 2\varphi(t), \tag{6.14}$$

where

$$\varphi(t) = \text{Im} \left[\tilde{A}(t)g(\eta(t)) \right] = \text{Im} \left[\frac{\eta'(t)}{\eta(t) - \beta} \right]. \tag{6.15}$$

By squaring both sides of (6.2) and dividing the result by $(\eta(t) - \beta)^2$, we obtain

$$\frac{\Phi(\eta(t))^2}{(\eta(t) - \beta)^2} = -\frac{R(t)^2}{(\eta(t) - \beta)^2} T(\eta(t))^2 \frac{\Phi'(\eta(t))^2}{|\Phi'(\eta(t))|^2}. \tag{6.16}$$

Upon comparing (6.16) with (3.2) leads to a choice of $P(\eta(t)) = \Phi(\eta(t))^2/(\eta(t) - \beta)^2$, $P(\infty) = 1$, $D(\eta(t)) = \Phi'(\eta(t))$, $D(\infty) = 1$, $c(t) = -R(t)^2/(\eta(t) - \beta)^2$. Hence,

$$\phi(t) = \Phi'(\eta(t))\eta'(t) \tag{6.17}$$

satisfies the integral equation (3.16) with

$$\nu(t) = -\frac{R(t)^2}{(\eta(t) - \beta)^2} \overline{\eta'(t)} + \eta'(t). \tag{6.18}$$

Numerical evidence shows that $\lambda = -1$ is an eigenvalue of $K(s, t)$ of multiplicity m , thus one needs to add m conditions. Since $\Phi(z)$ is assumed to be single-valued, it is also required that the unknown mapping function $\Phi'(z)$ satisfies [4]

$$\int_{J_j} \phi(t)dt = \int_{\Gamma_j} \Phi'(\eta)d\eta = 0, \quad j = 1, 2, \dots, m, \tag{6.19}$$

that is,

$$\mathbf{J}\phi = 0. \tag{6.20}$$

Then, $\phi(t)$ is the unique solution of the integral equation

$$(\mathbf{I} + \mathbf{K} + \mathbf{J})\phi(t) = \nu(t). \quad (6.21)$$

By obtaining $\phi(\eta(t))$, the derivatives of the mapping function, $\Phi'(t)$ can be obtained by

$$\Phi'(t) = \frac{\phi(\eta(t))}{\eta'(t)}. \quad (6.22)$$

7. Radial Slits

The canonical region U_r consists of m slits along m segments of the rays with $\arg(\Phi) = \theta_j$, $j = 1, 2, \dots, m$. Then, the boundary values of the mapping function Φ are given by

$$\Phi(\eta(t)) = r(t)e^{i\theta(t)} = e^{R(t)}e^{i\theta(t)}, \quad (7.1)$$

where the boundary correspondence function $\theta(t) = (\theta_1, \theta_2, \dots, \theta_m)$ now becomes real constant function and $R(t)$ is an unknown function. By taking logarithmic derivative on (7.1), we obtain

$$\eta'(t) \frac{\Phi'(\eta(t))}{\Phi(\eta(t))} = R'(t). \quad (7.2)$$

It can be shown that the mapping function $\Phi(z)$ can be determined using

$$\Phi(\eta(t)) = \frac{\eta'(t)\Phi'(\eta(t))}{R'(t)}. \quad (7.3)$$

The mapping function $\Phi(z)$ can be uniquely determined by assuming $\Phi(\beta) = 0$, $\Phi(\infty) = \infty$ and $\Phi'(\infty) = 1$. Thus, the mapping function $\Phi(z)$ can be expressed as [12]

$$\Phi(z) = (z - \beta)e^{iF(z)}. \quad (7.4)$$

By taking logarithm on both sides of (7.4) and multiplying the result by $-i$, we obtain

$$F(\eta(t)) = \theta - iR(t) + i\log(\eta(t) - \beta). \quad (7.5)$$

Hence, (7.5) satisfies boundary values in Theorem 2.1 with $A(t) = 1$,

$$h(t) = (\theta_1, \theta_2, \dots, \theta_m), \quad \gamma(t) = -\text{Arg}(\eta(t) - \beta). \quad (7.6)$$

By obtaining $h(t)$, one can obtain the values of $\theta(t)$ by

$$\theta_j = h_j \quad \text{for } j = 1, 2, \dots, m. \quad (7.7)$$

Then, by differentiating (7.5) and comparing with (7.2) yields

$$iR'(t) = -F'(\eta(t))\eta'(t) + i\frac{\eta'(t)}{\eta(t) - \beta}. \quad (7.8)$$

In view of $\tilde{A} = \eta'(t)$, $f(t) = F'(\eta(t))$ and $g(t) = i/(\eta(t) - \beta)$ where $f(z)$ is analytic in Ω^- and $g(z)$ is analytic in Ω^+ , we rewrite (7.8) as

$$\tilde{A}f(\eta(t)) = iR'(t) - \tilde{A}g(\eta(t)). \quad (7.9)$$

Let $\tilde{A}g(t) = \varphi + i\psi$. Then by [18, Theorems 2(c) and 2(d)], we obtain

$$\begin{aligned} (\mathbf{I} + \mathbf{N}^*)(\varphi(t) - R'(t)) &= -\tilde{\mathbf{M}}\varphi(t), \\ (\mathbf{I} - \mathbf{N}^*)\varphi(t) &= \tilde{\mathbf{M}}\varphi(t). \end{aligned} \quad (7.10)$$

Adding these equations, we get

$$(\mathbf{I} + \mathbf{N}^*)R'(t) = 2\varphi(t). \quad (7.11)$$

Since the images of the curve $\Gamma_1, \Gamma_2, \dots, \Gamma_m$ are slits, we have $R_j(2\pi) - R_j(0) = 0$. Therefore

$$\mathbf{J}R'(t) = (0, 0, \dots, 0). \quad (7.12)$$

Hence, the unknown function $R'(t)$ is the unique solution of the integral equation

$$(\mathbf{I} + \mathbf{N}^* + \mathbf{J})R'(t) = 2\varphi(t), \quad (7.13)$$

where

$$\varphi(t) = \text{Im} \left[\tilde{A}(t)g(\eta(t)) \right] = \text{Im} \left[\frac{i\eta'(t)}{\eta(t) - \beta} \right]. \quad (7.14)$$

The boundary relationship (7.3) can be rewritten as

$$\Phi'(\eta(t)) = \pm e^{i\theta_j} \overline{T(\eta(t))} |\Phi'(\eta(t))|. \quad (7.15)$$

Squaring both sides of (7.15) yields

$$\Phi'(\eta(t)) = e^{2i\theta_j} \overline{T(\eta(t))^2 \Phi'(\eta(t))}. \quad (7.16)$$

Upon comparing (7.16) with (3.1) leads to a choice of $P(\eta(t)) = 1$, $P(\infty) = 1$, $D(\eta(t)) = \Phi'(\eta(t))$, $D(\infty) = 1$, $c(t) = e^{i2\theta_j}$. Hence,

$$\phi(t) = \Phi'(\eta(t))\eta'(t) \quad (7.17)$$

satisfies the integral equation (3.16) with

$$\nu(t) = e^{2i\theta_j(t)}\overline{\eta'(t)} + \eta'(t). \quad (7.18)$$

Numerical evidence shows that $\lambda = -1$ is an eigenvalue of $K(s, t)$ of multiplicity m , which suggests one needs to add m conditions. Since $\Phi(z)$ is assumed to be single-valued, hence it is also required that the unknown mapping function $\Phi'(z)$ satisfies [4]

$$\int_{J_j} \phi(t)dt = \int_{\Gamma_j} \Phi'(\eta)d\eta = 0, \quad j = 1, 2, \dots, m, \quad (7.19)$$

that is,

$$\mathbf{J}\phi = 0. \quad (7.20)$$

Then, $\phi(t)$ is the solution of the following integral equation

$$(\mathbf{I} + \mathbf{K} + \mathbf{J})\phi(t) = \nu(t). \quad (7.21)$$

By obtaining $\phi(\eta(t))$, the derivatives of the mapping function $\Phi'(t)$ can be found using

$$\Phi'(t) = \frac{\phi(\eta(t))}{\eta'(t)}. \quad (7.22)$$

8. Parallel Slits

The canonical region U_p consists of a m parallel straight slits on the w -plane. Let $B = e^{i(\pi/2-\theta)}$, then the boundary values of the mapping function Φ are given by

$$B\Phi(\eta(t)) = R(t) + i\delta(t), \quad (8.1)$$

where θ is the angle of intersection between the lines $\text{Re}[B\Phi] = R_j$ and the real axis. $R(t) = (R_1(t), R_2(t), \dots, R_M(t))$ is a piecewise real constant function and $\delta(t)$ is an unknown function. It can be shown that (8.1) can be written as

$$B\Phi'(\eta(t))\eta'(t) = i\delta'(t). \quad (8.2)$$

The mapping function $\Phi(z)$ can be uniquely determined by assuming $\Phi(\infty) = \infty$ and $\lim_{z \rightarrow \infty} \Phi(z) - z = 0$. Thus, the mapping function Φ can be expressed as [12]

$$\Phi(z) = z + \bar{B}F(z), \tag{8.3}$$

where $F(z)$ is an analytic function with $F(\infty) = 0$. By multiplying both sides of (8.3) with B , we obtain

$$F(\eta(t)) = B\Phi(\eta(t)) - B\eta(t). \tag{8.4}$$

Hence, (8.4) satisfies the boundary values in Theorem 2.1 with $A(t) = 1$,

$$h(t) = (R_1, R_2, \dots, R_m) \quad \gamma(t) = -B\eta(t). \tag{8.5}$$

Differentiating (8.4) and comparing the result with (8.2) yield

$$i\delta'(t) = B\eta'(t) + \eta'(t)F'(\eta(t)). \tag{8.6}$$

In view of $\tilde{A} = \eta'(t)$, $f(t) = F'(\eta(t))$ and $g(t) = B$, where $f(z)$ is analytic in Ω^- and $g(z)$ is analytic in Ω^+ , we rewrite (8.6) as

$$\tilde{A}f(\eta(t)) = i\delta'(t) - \tilde{A}g(\eta(t)). \tag{8.7}$$

Assuming $\tilde{A}g(t) = \varphi + i\psi$, then by [18, Theorems 2(c) and 2(d)], we obtain

$$\begin{aligned} (\mathbf{I} + \mathbf{N}^*)(\delta'(t) - \varphi(t)) &= \tilde{\mathbf{M}}\psi(t), \\ (\mathbf{I} - \mathbf{N}^*)\varphi(t) &= \tilde{\mathbf{M}}\psi(t). \end{aligned} \tag{8.8}$$

These two equations yields

$$(\mathbf{I} + \mathbf{N}^*)\delta'(t) = 2\varphi(t). \tag{8.9}$$

Note that, the images of the curves $\Gamma_1, \Gamma_2, \dots, \Gamma_m$ are slits, so we have $\delta_j(2\pi) - \delta_j(0) = 0$, which implies

$$\mathbf{J}\delta'(t) = (0, 0, \dots, 0). \tag{8.10}$$

Hence, the unknown function $\delta'(t)$ is the unique solution of the integral equation

$$(\mathbf{I} + \mathbf{N}^* + \mathbf{J})\delta'(t) = 2\varphi(t), \tag{8.11}$$

where

$$\varphi(t) = \operatorname{Im} \left[\tilde{A}(t)g(\eta(t)) \right] = \operatorname{Im} [\eta'(t)B]. \quad (8.12)$$

From (8.1), we introduce an analytic function $\vartheta(\eta(t))$ such that

$$\vartheta(\eta(t)) = e^{F(z)} = e^{-B\eta(t)} e^{R(t)+i\delta(t)}, \quad (8.13)$$

where $\vartheta(\infty) = 1$. By differentiating (8.13) with respect to t , we obtain

$$\vartheta'(\eta(t))\eta'(t) = (i\delta'(t) - B\eta'(t))\vartheta(\eta(t)). \quad (8.14)$$

Let $\sigma(t)$ be an analytic function such that it has the following representation

$$\sigma(\eta(t)) = \vartheta'(\eta(t)) + B\vartheta(\eta(t)), \quad (8.15)$$

where $\sigma(\infty) = B$. From (8.13)–(8.15) it can be shown that, the function $\vartheta(\eta(t))$ can be rewritten as

$$\vartheta(\eta(t)) = e^{R_j} e^{(-\operatorname{Re}[B\eta(t)])} \frac{\operatorname{sign}(\delta'(t))}{i} T(\eta(t)) \frac{\sigma(\eta(t))}{|\sigma(\eta(t))|}. \quad (8.16)$$

By squaring both sides of (8.16), the sign $\delta'(t)$ is eliminated, that is,

$$\vartheta(\eta(t))^2 = -e^{2R_j} e^{(-2\operatorname{Re}[B\eta(t)])} T(\eta(t))^2 \frac{\sigma(\eta(t))^2}{|\sigma(\eta(t))|^2}. \quad (8.17)$$

Comparing (8.17) with (3.2) leads to a choice of $P(z) = \vartheta(z)^2$, $P(\infty) = 1$, $D(z) = \sigma(z)$, $D(\infty) = B$, $c(t) = -e^{2R_j} e^{(-2\operatorname{Re}[B\eta(t)])}$. Hence,

$$\phi(t) = \sigma(\eta(t))\eta'(t) \quad (8.18)$$

satisfies the integral equation (3.16) with

$$\nu(t) = -e^{2R_j} e^{(-2\operatorname{Re}[B\eta(t)])} \overline{\eta'(t)B} + B\eta'(t). \quad (8.19)$$

Numerical evidence shows that $\lambda = -1$ is an eigenvalue of $K(s, t)$ of multiplicity m , which suggests one needs to add m conditions. Since $e^{B\eta_j(t)}\vartheta(\eta_j(t))|_0^{2\pi} = 0$, hence we can have m additional conditions for the integral equation above as in the following:

$$\begin{aligned} \int_{J_j} \frac{d}{dt} \left(e^{B\eta_j(t)} \vartheta_j(\eta_j(t)) \right) dt &= 0, \\ \int_0^{2\pi} e^{B\eta_j(t)} \left(\vartheta'_j(\eta_j(t)) + B\vartheta(\eta_j(t)) \right) \eta'_j(t) dt &= 0, \\ \int_0^{2\pi} e^{B\eta_j(t)} (\sigma(\eta_j(t))) \eta'_j(t) dt &= 0, \\ \int_0^{2\pi} e^{B\eta_j(t)} \phi(\eta_j(t)) dt &= 0, \quad q = 1, 2, \dots, m. \end{aligned} \tag{8.20}$$

We define Fredholm operator \mathbf{L} as

$$\mathbf{L}\mu(s) = \int_{J_j} e^{B\eta_j(t)} \mu(t) dt. \tag{8.21}$$

Then, $\phi(t)$ is the solution of the following integral equation:

$$(\mathbf{I} + \mathbf{K} + \mathbf{L})\phi(t) = \nu(t). \tag{8.22}$$

Hence, by obtaining $\phi(\eta(t))$, the function $\sigma(t)$ can be found by

$$\sigma(t) = \frac{\phi(\eta(t))}{\eta'(t)}. \tag{8.23}$$

This allows the value for $\vartheta(\eta(t))$ to be calculated from (8.16), which in turn allows the boundary values for the mapping function $\Phi(\eta(t))$ to be calculated by

$$\Phi(\eta(t)) = \eta(t) + \bar{B} \log \vartheta(\eta(t)). \tag{8.24}$$

9. Numerical Examples

Since the boundaries Γ_j are parameterized by $\eta(t)$ which are 2π -periodic functions, the reliable method to solve the integral equations are by means of Nyström method with trapezoidal rule [21]. Each boundary will be discretized by n number of equidistant points. The resulting linear systems are then solved by using Gaussian elimination. For numerical examples, we choose regions with connectivities one, two, three and four. For the region

Table 1: Error norm $\|w_j - \hat{w}_j\|_\infty$ for Example 9.1.

n	U_c	U_r	$U_{p,\pi/3}$
32	6.2×10^{-12}	4.6×10^{-14}	8.8×10^{-16}
64	9.1×10^{-14}	9.6×10^{-15}	—

with connectivity one, we compare our result with the analytic solution given in [12]. All the computations were done by using MATLAB R2008a software.

Example 9.1. Consider an unbounded region Ω^- bounded by a unit circle

$$\Gamma_1(t) = e^{-it}, \quad (0 \leq t \leq 2\pi). \quad (9.1)$$

We choose the special point $\beta = 2.5 + 1.5i$. The exact mapping function for U_c, U_r , and U_p are given respectively by [12]

$$\begin{aligned} w_c &= z - \beta + \frac{\beta - z}{1 - \beta z}, \\ w_r &= z - \beta - \frac{z - \beta}{\beta z}, \\ w_p &= z + \frac{e^{2i\theta}}{z}. \end{aligned} \quad (9.2)$$

For this example, we compare the error for each boundary value between our method and the exact mapping function. See Table 1 for Error Norm of $\|w_j - \hat{w}_j\|_\infty$.

Example 9.2. Consider an unbounded region Ω^- bounded by a circle and an ellipse

$$\begin{aligned} \Gamma_1(t) &= 2 + i + e^{-it}, \quad (0 \leq t \leq 2\pi), \\ \Gamma_2(t) &= -2 + \cos t - 2i \sin t, \quad (0 \leq t \leq 2\pi). \end{aligned} \quad (9.3)$$

Figure 2 shows the region and its five canonical images by using our proposed method.

Example 9.3. Consider an unbounded region Ω^- bounded by 3 circles

$$\begin{aligned} \Gamma_1(t) &= 2 + e^{-it}, \quad (0 \leq t \leq 2\pi), \\ \Gamma_2(t) &= -1 + i\sqrt{3} + 0.5e^{-it}, \quad (0 \leq t \leq 2\pi), \\ \Gamma_3(t) &= -1 - i\sqrt{3} + 1.5e^{-it}, \quad (0 \leq t \leq 2\pi). \end{aligned} \quad (9.4)$$

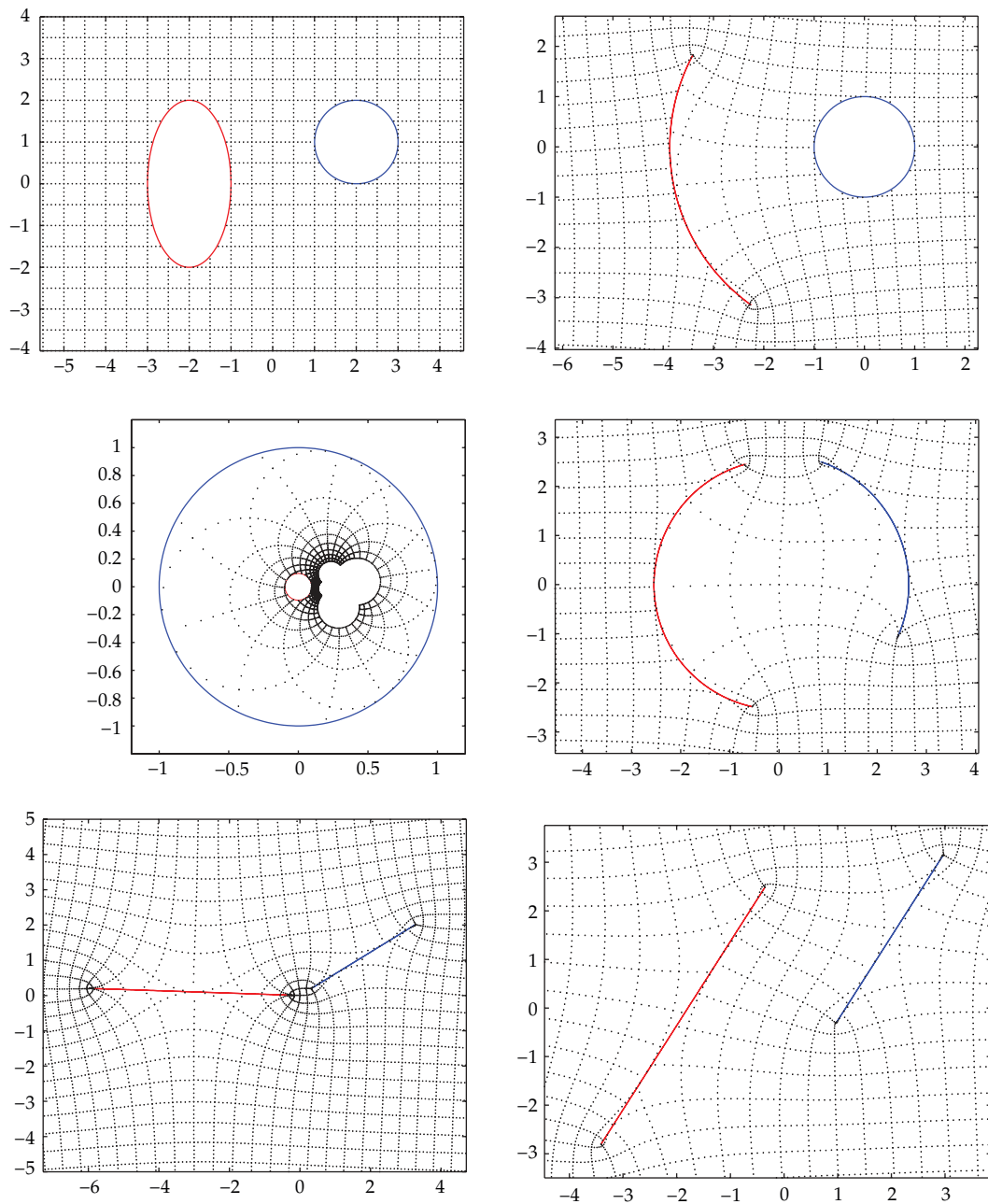


Figure 2: The original region Ω^- and its canonical images with $\theta_p = \pi/3$ for parallel slits.

This example has also been considered in [6, 12]. Figure 3 shows the regions and its five canonical images by using our proposed method. See Table 3 for numerical comparison between our parameter values (see Table 2) those in [12]. Note that our method has considered exterior unit disk with slits as a canonical region while [12] has considered interior

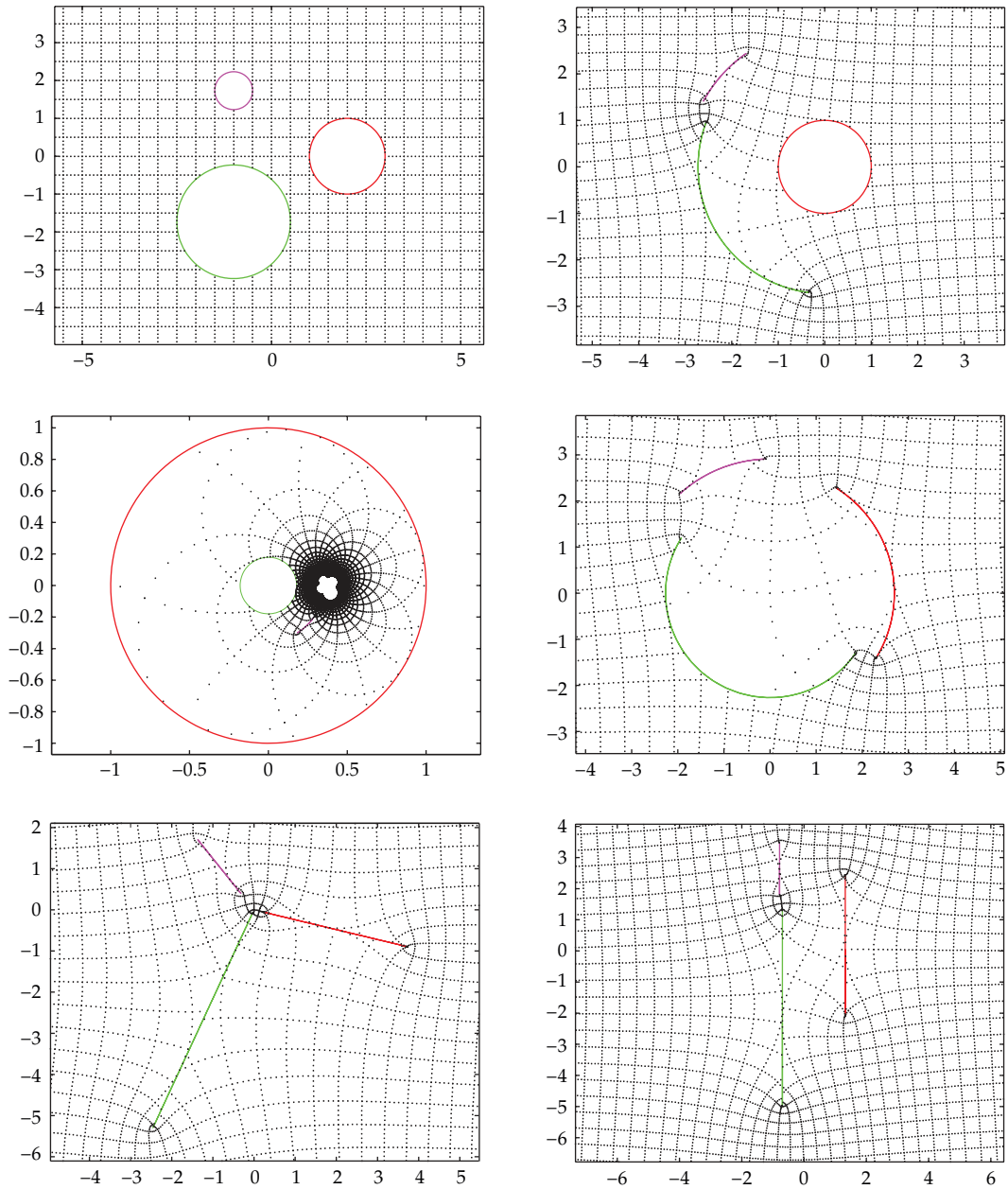


Figure 3: The original region Ω^- and its canonical images with $\theta_p = \pi/2$ for parallel slits.

unit disk with slits. Thus, in computing the error for U_d , we need to change the values for U_d to $1/|\Phi(z)|$. See Table 4 for Error Norm of $\max_{1 \leq j \leq 3} \|w_j - \hat{w}_j\|_\infty$. We also compared the condition number of our linear system for each n with [6, 12], see Figures 4 and 5. The results show that for our integral equations for finding $\Phi'(z)$ that is, (4.20), (5.20), (6.21), (7.21) and (8.22), the condition numbers are almost constant except for (5.20). This is because the kernel

Table 2: The values for approximated parameters in Example 9.3 with $n = 256$.

j	$R_j(U_d)$	$R_j(U_a)$	$R_j(U_c)$	$\theta_j(U_r)$	$R_j(U_{p,\pi/2})$
1	1.0000000000	1.0000000000	2.6958524041	-0.23582974094	1.32203173492
2	2.9672620504	0.3515929850	2.9121788457	2.24673051228	-0.78705294688
3	2.7249636495	0.1792099292	2.2653736950	-2.00502589294	-0.69725704737

Table 3: Error norm $\max_{1 \leq j \leq 3} \|R_j - \hat{R}_j\|_\infty$ of our method with [12] for Example 9.3.

n	U_d	U_a	U_c	U_r	$U_{p,\pi/2}$
32	2.7×10^{-11}	3.4×10^{-11}	2.9×10^{-01}	1.6×10^{-01}	2.0×10^{-10}
64	5.6×10^{-17}	1.1×10^{-16}	4.4×10^{-05}	2.0×10^{-05}	2.2×10^{-16}
128	7.8×10^{-16}	4.7×10^{-16}	2.2×10^{-09}	4.1×10^{-10}	8.9×10^{-16}
256	1.6×10^{-15}	9.99×10^{-16}	3.8×10^{-12}	5.2×10^{-13}	1.3×10^{-15}

Table 4: Error norm $\max_{1 \leq j \leq 3} \|w_j - \hat{w}_j\|_\infty$ of our method with [12] for Example 9.3.

n	U_d	U_a	U_c	U_r	$U_{p,\pi/2}$
32	1.1×10^{-07}	1.1×10^{-07}	0.15	0.16	1.5×10^{-06}
64	6.1×10^{-14}	2.9×10^{-14}	6.2×10^{-05}	2.0×10^{-05}	1.1×10^{-13}
128	7.5×10^{-14}	2.1×10^{-14}	2.2×10^{-09}	4.2×10^{-10}	4.4×10^{-12}
256	2.2×10^{-13}	4.7×10^{-13}	3.3×10^{-12}	4.1×10^{-12}	9.5×10^{-12}

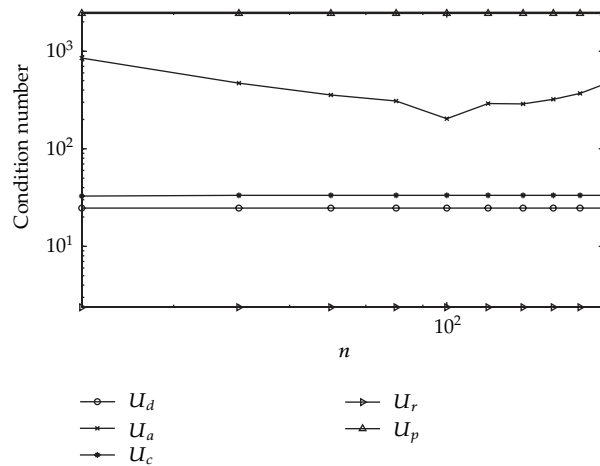


Figure 4: Condition numbers of the matrices for our method for U_d, U_a, U_c, U_r and U_p .

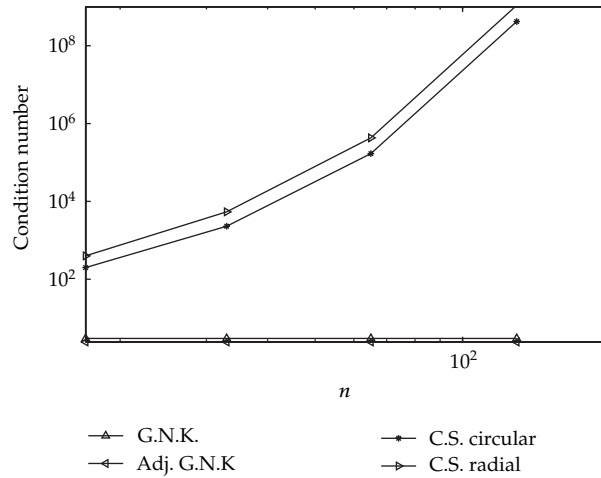


Figure 5: Condition number of the matrices for generalized Neumann kernel (G.N.K), adjoint generalized Neumann kernel (Adj.G. N. K), charge simulation for circular slits (C.S. circular) and charge simulation for radial slits (C.S. radial).

involves $\theta'(t)$, which varies with the number of collocation points, n . However, this does not have any effect on the accuracy of the method.

Example 9.4. Consider an unbounded region Ω^- of 4-connectivity with boundaries

$$\Gamma_1(t) = 3 + 2i + e^{-it}, \quad (0 \leq t \leq 2\pi), \quad (9.5)$$

$$\Gamma_2(t) = -3 + 2i + e^{-it}, \quad (0 \leq t \leq 2\pi), \quad (9.6)$$

$$\Gamma_3(t) = -3 - 2i + 0.7 \cos t - 1.4i \sin t, \quad (0 \leq t \leq 2\pi), \quad (9.7)$$

$$\Gamma_4(t) = 3 - 2i + 0.7 \cos t - 1.4i \sin t, \quad (0 \leq t \leq 2\pi). \quad (9.8)$$

Figure 6 shows the region and its five canonical images by using our proposed method.

10. Conclusion

In this paper, we have constructed a unified method for numerical conformal mapping of unbounded multiply connected regions onto canonical slit regions. The advantage of this method is that the integral equations are all linear which overcomes the nonlinearity problem encountered in [10]. From the numerical experiments, we can conclude that our method works on any finite connectivity with high accuracy. By computing the boundary values of the mapping function, the exterior points will be calculated by means of Cauchy's integral formula.

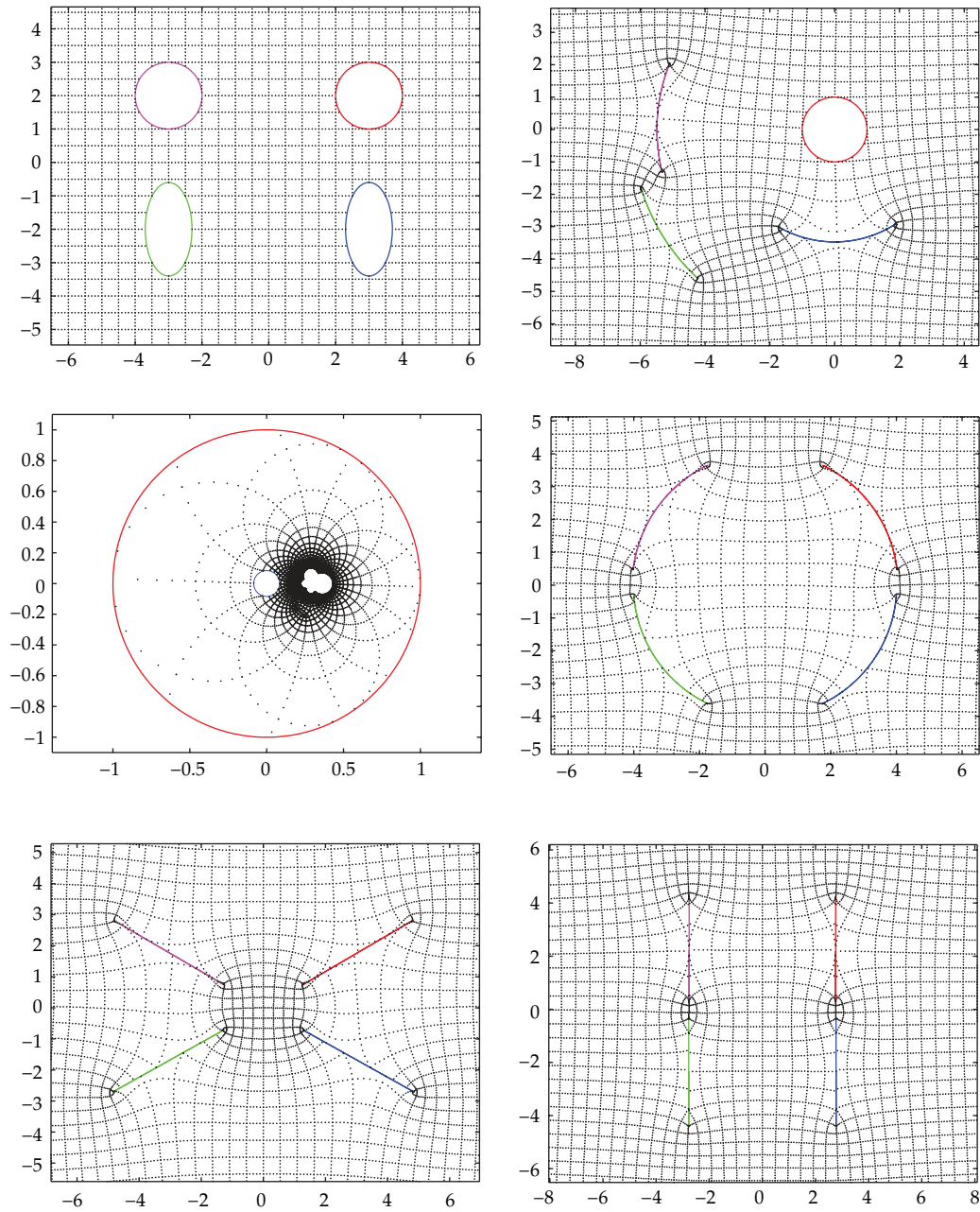


Figure 6: The original region Ω^- and its canonical images with $\theta_p = \pi/2$ for parallel slits.

Acknowledgments

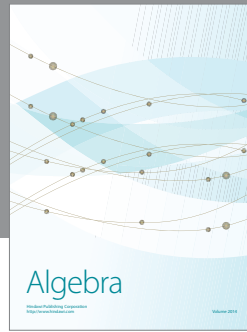
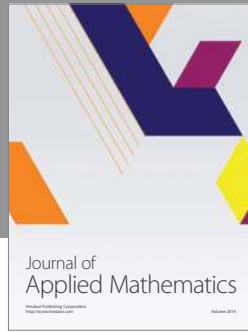
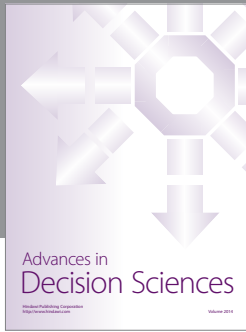
This work was supported in part by the Malaysian Ministry of Higher Education (MOHE) through the Research Management Centre (RMC), Universiti Teknologi Malaysia (GUP Q.J130000.7126.01H75). This support is gratefully acknowledged. The authors would like

to thank the anonymous referees for their valuable comments and suggestions on the manuscript which improved the presentation of the paper.

References

- [1] V. V. Andreev, D. Daniel, and T. H. McNicholl, "Technical report: Computation on the extended complex plane and conformal mapping of multiply-connected domains," in *Proceedings of the 5th International Conference on Computability and Complexity in Analysis (CCA '08)*, vol. 221 of *Electronic Notes in Theoretical Computer Science*, pp. 127–139, Elsevier, 2008.
- [2] G. C. Wen, *Conformal Mapping and Boundary Values Problems*, vol. 106 of *Translations of Mathematical Monographs*, American Mathematical Society, Providence, RI, USA, 1992, English translation of Chinese edition, 1984.
- [3] Z. Nehari, *Conformal Mapping*, Dover, New York, NY, USA, 1952.
- [4] P. Henrici, *Applied and Computational Complex Analysis. Vol. 3*, Pure and Applied Mathematics, John Wiley & Sons, New York, NY, USA, 1986.
- [5] L. N. Trefethen, Ed., *Numerical Conformal Mapping*, North-Holland, Amsterdam, The Netherlands, 1986.
- [6] K. Amano, "A charge simulation method for numerical conformal mapping onto circular and radial slit domains," *SIAM Journal on Scientific Computing*, vol. 19, no. 4, pp. 1169–1187, 1998.
- [7] T. K. DeLillo, T. A. Driscoll, A. R. Elcrat, and J. A. Pfaltzgraff, "Radial and circular slit maps of unbounded multiply connected circle domains," *Proceedings of The Royal Society of London Series A*, vol. 464, no. 2095, pp. 1719–1737, 2008.
- [8] A. H. M. Murid, *Boundary integral equation approach for numerical conformal mapping [Ph.D. thesis]*, Universiti Teknologi Malaysia, 1999.
- [9] A. H. M. Murid and M. R. M. Razali, "An integral equation method for conformal mapping of doubly connected regions," *Matematika*, vol. 15, no. 2, pp. 79–93, 1999.
- [10] A. H. M. Murid and L.-N. Hu, "Numerical experiment on conformal mapping of doubly connected regions onto a disk with a slit," *International Journal of Pure and Applied Mathematics*, vol. 51, no. 4, pp. 589–608, 2009.
- [11] M. M. S. Nasser, "A boundary integral equation for conformal mapping of bounded multiply connected regions," *Computational Methods and Function Theory*, vol. 9, no. 1, pp. 127–143, 2009.
- [12] M. M. S. Nasser, "Numerical conformal mapping via a boundary integral equation with the generalized Neumann kernel," *SIAM Journal on Scientific Computing*, vol. 31, no. 3, pp. 1695–1715, 2009.
- [13] M. M. S. Nasser, "Numerical conformal mapping of multiply connected regions onto the second, third and fourth categories of Koebe's canonical slit domains," *Journal of Mathematical Analysis and Applications*, vol. 382, no. 1, pp. 47–56, 2011.
- [14] A. W. K. Sangawi, A. H. M. Murid, and M. M. S. Nasser, "Linear integral equations for conformal mapping of bounded multiply connected regions onto a disk with circular slits," *Applied Mathematics and Computation*, vol. 218, no. 5, pp. 2055–2068, 2011.
- [15] A. W. K. Sangawi, A. H. M. Murid, and M. M. S. Nasser, "Annulus with circular slit map of bounded multiply connected regions via integral equation method," *Bulletin of Malaysian Mathematical Sciences Society*. In press.
- [16] A. W. K. Sangawi, A. H. M. Murid, and M. M. S. Nasser, "Circular slits map of bounded multiply connected regions," *Abstract and Applied Analysis*, vol. 2012, Article ID 970928, 26 pages, 2012.
- [17] A. W. K. Sangawi, A. H. M. Murid, and M. M. S. Nasser, "Parallel slits map of bounded multiply connected regions," *Journal of Mathematical Analysis and Applications*, vol. 389, no. 2, pp. 1280–1290, 2012.
- [18] R. Wegmann and M. M. S. Nasser, "The Riemann-Hilbert problem and the generalized Neumann kernel on multiply connected regions," *Journal of Computational and Applied Mathematics*, vol. 214, no. 1, pp. 36–57, 2008.
- [19] M. M. S. Nasser, A. H. M. Murid, M. Ismail, and E. M. A. Alejaily, "Boundary integral equations with the generalized Neumann kernel for Laplace's equation in multiply connected regions," *Applied Mathematics and Computation*, vol. 217, no. 9, pp. 4710–4727, 2011.

- [20] F. D. Gakhov, *Boundary Value Problems*, Translation edited by I. N. Sneddon, Pergamon Press, Oxford, UK, 1966, English translation of Russian edition, 1963.
- [21] K. E. Atkinson, *The Numerical Solution of Integral Equations of the Second Kind*, vol. 4 of *Cambridge Monographs on Applied and Computational Mathematics*, Cambridge University Press, Cambridge, UK, 1997.



Hindawi

Submit your manuscripts at
<http://www.hindawi.com>

